



Calhoun: The NPS Institutional Archive

Theses and Dissertations

Thesis Collection

1994-06

Trim effects on motion stability of submersible vehicles

Örnek, Selçuk

Monterey, California. Naval Postgraduate School

<http://hdl.handle.net/10945/28617>



Calhoun is a project of the Dudley Knox Library at NPS, furthering the precepts and goals of open government and government transparency. All information contained herein has been approved for release by the NPS Public Affairs Officer.

Dudley Knox Library / Naval Postgraduate School
411 Dyer Road / 1 University Circle
Monterey, California USA 93943

<http://www.nps.edu/library>

DUDLEY KNOX LIBRARY
NAVAL POSTGRADUATE SCHOOL
MONTAGUE, CA 93943-5101

Approved for public release; distribution is unlimited.

TRIM EFFECTS ON MOTION STABILITY
OF SUBMERSIBLE VEHICLES

by

Selçuk Örnek

Lieutenant Junior Grade, Turkish Navy

B.S., Turkish Naval Academy, 1988

Submitted in partial fulfillment
of the requirements for the degree of

MASTER OF SCIENCE IN MECHANICAL ENGINEERING

from the

NAVAL POSTGRADUATE SCHOOL

June 1994

REPORT DOCUMENTATION PAGE

Form Approved OMB No. 0704-0188

Public reporting burden for this collection of information is estimated to average 1 hour per response, including the time for reviewing instruction, searching existing data sources, gathering and maintaining the data needed, and completing and reviewing the collection of information. Send comments regarding this burden estimate or any other aspect of this collection of information, including suggestions for reducing this burden, to Washington Headquarters Services, Directorate for Information Operations and Reports, 1215 Jefferson Davis Highway, Suite 1204, Arlington, VA 22202-4302, and to the Office of Management and Budget, Paperwork Reduction Project (0704-0188) Washington DC 20503.

1. AGENCY USE ONLY (Leave blank)		2. REPORT DATE 7 June 1994	3. REPORT TYPE AND DATES COVERED Master's Thesis	
4. TITLE AND SUBTITLE TRIM EFFECTS ON MOTION STABILITY OF SUBMERSIBLE VEHICLES			5. FUNDING NUMBERS	
6. AUTHOR(S) ÖRNEK Selçuk				
7. PERFORMING ORGANIZATION NAME(S) AND ADDRESS(ES) Naval Postgraduate School Monterey CA 93943-5000			8. PERFORMING ORGANIZATION REPORT NUMBER	
9. SPONSORING/MONITORING AGENCY NAME(S) AND ADDRESS(ES)			10. SPONSORING/MONITORING AGENCY REPORT NUMBER	
11. SUPPLEMENTARY NOTES The views expressed in this thesis are those of the author and do not reflect the official policy or position of the Department of Defense or the U.S. Government.				
12a. DISTRIBUTION/AVAILABILITY STATEMENT Approved for public release; distribution is unlimited.			12b. DISTRIBUTION CODE A	
13. ABSTRACT The effects of trim on stability of motion during depth control of submersible vehicles are analysed. Full state feedback control is used to provide stable response in the dive plane, and feedforward control is used to ensure steady state accuracy. A complete set of stability maps is generated for various values of metacentric height, longitudinal center of gravity/center of buoyancy separation, forward speed, and control law time constant. The results clearly indicate ranges of parameters that should be chosen in design and operation of a given vehicle.				
14. SUBJECT TERMS Submarine, bifurcation, out of trim			15. NUMBER OF PAGES 59	
			16. PRICE CODE	
17. SECURITY CLASSIFICATION OF REPORT Unclassified	18. SECURITY CLASSIFICATION OF THIS PAGE Unclassified	19. SECURITY CLASSIFICATION OF ABSTRACT Unclassified	20. LIMITATION OF ABSTRACT UL	

NSN 7540-01-280-5500

Standard Form 298 (Rev. 2-89)

Prescribed by ANSI Std. Z39-18

ABSTRACT

The effects of trim on stability of motion during depth control of submersible vehicles are analysed. Full state feedback control is used to provide stable response in the dive plane, and feedforward control is used to ensure steady state accuracy. A complete set of stability maps is generated for various values of metacentric height, longitudinal center of gravity/center of buoyancy separation, forward speed, and control law time constant. The results clearly indicate ranges of parameters that should be chosen in design and operation of a given vehicle.

Thesis
05866
c.1

TABLE OF CONTENTS

I.	INTRODUCTION	1
II.	EQUATIONS OF MOTION	2
III.	CONTROL LAW	7
	A. INTRODUCTION	7
	B. FEEDBACK CONTROL	8
	1. Pole Placement	8
	2. Pole Location Selection	10
	C. FEEDFORWARD CONTROL	11
IV.	BIFURCATION ANALYSIS	16
	A. STABILITY	16
	B. BIFURCATION	17
	C. RESULTS AND DISCUSSION	19
V.	CONCLUSIONS AND RECOMMENDATIONS	35
	A. CONCLUSIONS	35
	B. RECOMMENDATIONS	36
	APPENDIX BIFURCATION ANALYSIS PROGRAM	37

LIST OF REFERENCES 50

INITIAL DISTRIBUTION LIST 51

NOMENCLATURE

<u>Symbol:</u>	<u>Definition:</u>
A	Closed loop dynamics matrix for the linearized system
α	Control surface coordination gain
$b(x)$	Local beam of the hull
B	Vehicle buoyancy
B	Control matrix in state space
C_D	Quadratic drag coefficient
c_1, c_2	Coupled heave and pitch terms
d_q, d_w	Cross flow drag terms
δ_b	Bow plane deflection
δ_s, δ	Stern plane deflection
I_y	Vehicle mass moment of inertia
I_H, I_P	Cross flow drag terms
k_1, k_2, k_3, k_4	Controller gains in θ, w, q , and z
K_0	Feedforward gain
m	Vehicle mass
M	Pitch moment
M_a	Partial derivative of M w.r.t. a
θ	Pitch angle
q	Pitch rate
T_c	Time constant
U	Forward speed
U_o	Nominal speed
w	Heave velocity
W	Vehicle weight
x	State vector
x_B, z_B	Body fixed coordinates of vehicle center of buoyancy
x_G, z_G	Body fixed coordinates of vehicle center of gravity
z	Deviation off the nominal depth
z_{GB}	Vehicle metacentric height
Z	Heave force
Z_a	Partial derivative of Z w.r.t. a

I. INTRODUCTION

The fundamental goal of submarine control is to reach and maintain ordered depth. Experimental designs involve expensive model testing such as Darpa Suboff Model (DTRC Model 5470) [Ref. 6]. Much research has been done in depth control of submarines [Ref. 3,5]. Our goal is to develop an analytic method to determine the stability properties of a design.

The stability of a design will have a significant impact on its responsiveness. A vehicle with a large margin to instability will not be very responsive. The problem becomes one of determining how close to the margins we can get without a total loss of stability. By expanding the scope of our research to include nonlinear terms we are able to define the limits of stability and therefore margins.

Previous studies analyzed stability properties of the system, specially static bifurcations [Ref. 2] and bifurcations to periodic solutions [Ref. 1]. The latter study which is used as a basis for this work, was restricted to level, zero trim flight paths.

The purpose of this thesis is to develop a program for finding the limits of stability for an out of trim submarine at moderate and high speeds. These limits are mapped using a Hopf bifurcation analysis program included in the Appendix.

II. EQUATIONS OF MOTION

The motion of the submersible in the vertical plane can be modeled by four coupled nonlinear differential equations for pitch rate (q), heave velocity (w), pitch angle (θ) and heave (z). With a body fixed coordinate frame at the vehicle's geometric center, we can express Newton's equations of motion as

$$m(\dot{w} - Uq - z_G \dot{q}^2 - x_G \dot{q}) = Z_q \dot{q} + Z_w \dot{w} + Z_{\delta_b} \delta_b + Z_s \delta_s + Z_w w + Z_q q - \frac{I}{2} \rho \int C_D b(x) \frac{(w - xq)^3}{|w - xq|} dx \quad (2.1)$$

$$I_y - m x_G (\dot{w} - Uq) - z_G w q m = -x_{GB} B \cos \theta - z_{GB} B \sin \theta + M_{\delta_s} \delta_s + M_{\delta_b} \delta_b + M_q \dot{q} + M_w \dot{w} + M_q q + M_w w + \frac{I}{2} \rho \int C_D b(x) \frac{(w - xq)^3}{|w - xq|} x dx \quad (2.2)$$

$$\dot{\theta} = q \quad (2.3)$$

$$\dot{z} = -U \sin \theta + w \cos \theta \quad (2.4)$$

Equations 2.1 through 2.2 can be written in a more compact form as,

$$\dot{w} = a_{11}Uw + a_{12}Uq + a_{13}z_{GB}\sin\theta + a_{13}x_{GB}\cos\theta + b_1U^2\delta_s + b_2U^2\delta_b + d_w(w,q) + c_1(w,q) \quad (2.5)$$

$$\dot{q} = a_{21}Uw + a_{22}Uq + a_{23}z_{GB}\sin\theta + a_{23}x_{GB}\cos\theta + b_1U^2\delta_s + b_2U^2\delta_b + d_q(w,q) + c_2(w,q) \quad (2.6)$$

where,

$$D_v = (m - Z_w)(I_y - M_q) - (mx_G + Z_q)(mx_G + M_w)$$

$$a_{11}D_v = (Z_w - 2C_DE_0U\tan\theta_0)(I_y - M_q) + (mx_G + Z_q)(M_w + 2C_DE_1U\tan\theta_0)$$

$$a_{12}D_v = (m + Z_q + 2C_DE_1U\tan\theta_0)(I_y - M_q) + (mx_G + Z_q)(M_q - mx_G - mz_GU\tan\theta_0 - 2C_DE_2U\tan\theta_0)$$

$$a_{21}D_v = (M_w + 2C_DE_1U\tan\theta_0)(m - Z_w) + (mx_G + M_w)(Z_w - 2C_DE_0U\tan\theta_0)$$

$$a_{22}D_v = (M_q - mx_G - mz_GU\tan\theta_0 - 2C_DE_2U\tan\theta_0)(mx_G + M_w)(m + Z_q + 2C_DE_1U\tan\theta_0)$$

(2.7)

$$a_{23}D_v = -(m + Z_w)B$$

$$a_{13}D_v = -(mx_G + Z_q)B$$

$$b_1D_v = (I_y - M_q)Z_\delta - (x_G + Z_q)M_\delta$$

$$b_2 D_v = (m - Z_w) M_\delta + (mx_G + M_w) Z_\delta$$

$$d_q(w, q) D_v = (m - Z_w) I_q + (mx_G + M_w) I_w$$

$$d_w(w, q) D_v = (I_y - M_q) I_w - (mx_G + Z_q) I_q$$

$$c_1(w, q) D_v = (I_y - M_q) m z_G q^2 - (mx_G + Z_q) m z_G w q$$

$$c_2(w, q) D_v = - (m - Z_w) m z_G w q - (mx_G + M_w) m z_G q^2$$

In these equations the submersible is assumed to be neutrally buoyant ($W=B$), and statically stable ($z_G > z_B$). Here we can assume z_B to be zero, hence $z_{GB} = z_G$.

At steady state the cross flow drag integral terms I_H and I_P have the form,

$$I_H = -C_D w |w| \int b(x) dx \quad I_P = C_D w |w| \int b(x) x dx \quad (2.8)$$

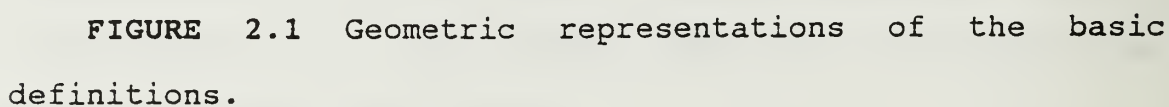
From equation (2.3) it is seen that w is equal to $\tan\theta_0$ at steady state. The $\int b(x) dx$ term is computed numerically for the SUBOFF model as E_0 , and $\int b(x) x dx$ term as E_1 . Therefore, the cross flow drag terms become,

$$I_H = -C_D w |w| E_0 \quad I_P = C_D w |w| E_1 \quad (2.9)$$

Because we have two rudders at the bow and the stern, our system of equations is multi-input. To reduce this system into a single input system the linear combination of the control inputs will be modified into the following form,

$$\delta = \delta_s \quad , \quad \delta_b = \alpha \delta_s \quad (2.10)$$

where α is the control surface coordination gain. The value of α ranges from -1 to 1. The selection of the value of α will allow the planes to operate as desired for the particular maneuvering condition, i.e., $\alpha = 0$ for no bow plane control, $\alpha = -1$ for bow plane and stern plane opposed to each other, yielding the maximum pitch moment, and $\alpha = 1$ for bow and stern plane control in the same direction, yielding the maximum heave force.



III. CONTROL LAW

A. INTRODUCTION

The control design problem can be expressed in state space as follows,

$$\dot{x} = Ax + B\delta \quad (3.1)$$

where the state vector is

$$x = \begin{bmatrix} \theta \\ w \\ q \\ z \end{bmatrix} \quad (3.2)$$

Equation 3.1 in our case is,

$$\begin{bmatrix} \dot{\theta} \\ \dot{w} \\ \dot{q} \\ \dot{z} \end{bmatrix} = \begin{bmatrix} 0 & 0 & 1 & 0 \\ a_{13}z_{GB} - b_1u^2k_1 & a_{11}u - b_1u^2k_2 & a_{12}u - b_1u^2k_3 & -b_1u^2k_4 \\ a_{23}z_{GB} - b_2u^2k_1 & a_{21}u - b_2u^2k_2 & a_{22}u - b_2u^2k_3 & -b_2u^2k_4 \\ -u & 1 & 0 & 0 \end{bmatrix} \begin{bmatrix} \theta \\ w \\ q \\ z \end{bmatrix} \quad (3.3)$$

Our aim is to find a controller which will assure us a stable closed loop system. The only control input is the dive plane angle, δ .

B. FEEDBACK CONTROL

1. Pole Placement

The full state feedback controller is a linear function of the states and has the form,

$$\delta = -Kx \quad (3.4)$$

where K is the vector of feedback gains which are to be determined in order to give the desired closed loop system dynamics. Substituting equation 2.12 into 2.10 yields,

$$\dot{x} = (A - BK)x \quad (3.5)$$

The feedback gains K must be chosen such that $A - BK$ has the desired eigenvalues. The actual characteristic equation of the closed loop system is given by,

$$\det(A - BK - sI) = 0 \quad (3.6)$$

The required values of K are obtained by matching coefficients in the two polynomials of the actual and the desired characteristic equations. Equation 3.5 becomes,

$$\begin{bmatrix} \dot{\theta} \\ \dot{w} \\ \dot{q} \\ \dot{z} \end{bmatrix} = \begin{bmatrix} 0 & 0 & 1 & 0 \\ a_{13}z_{GB} & a_{11}u & a_{12}u & 0 \\ a_{23}z_{GB} & a_{21}u & a_{22}u & 0 \\ -u & 1 & 0 & 0 \end{bmatrix} \begin{bmatrix} \theta \\ w \\ q \\ z \end{bmatrix} + \begin{bmatrix} 0 \\ b_1u^2 \\ b_2u^2 \\ 0 \end{bmatrix} \delta \quad (3.7)$$

The characteristic equation of the closed loop system is,

$$\det \begin{bmatrix} -s & 0 & 1 & 0 \\ a_{13}z_{GB} - b_1 u^2 k_1 & a_{11}u - b_1 u^2 k_2 - s & a_{12}u - b_1 u^2 k_3 & -b_1 u^2 k_4 \\ a_{23}z_{GB} - b_2 u^2 k_1 & a_{21}u - b_2 u^2 k_2 & a_{22}u - b_2 u^2 k_3 - s & -b_2 u^2 k_4 \\ -u & 1 & 0 & -s \end{bmatrix} \quad (3.8)$$

which reduces to,

$$s^4 + (A_2 k_2 + A_3 k_3 - E_1) s^3 + (-B_1 k_1 - B_2 k_2 - B_3 k_3 - B_4 k_4 - E_2) s^2 + (-C_1 k_1 - C_2 k_2 - C_3 k_3 - E_3) s + (-D_1 k_4 - D_2 k_4) = 0 \quad (3.9)$$

where,

$$\begin{aligned} A_2 &= -B_4 = b_1 u^2 \\ A_3 &= -B_1 = b_2 u^2 \\ B_2 &= (a_{22} b_1 - a_{12} b_2) u^3 \\ B_3 &= C_1 = (a_{11} b_2 - a_{21} b_1) u^3 \\ C_2 &= D_1 = (a_{23} b_1 - a_{13} b_2) z_{GB} u^2 \\ C_4 &= (a_{22} b_1 + b_2 - a_{12} b_2) u^3 \\ D_2 &= (a_{11} b_2 - a_{21} b_1) u^4 \\ E_1 &= (a_{11} + a_{22}) u \\ E_2 &= a_{23} z_{GB} + (a_{12} a_{21} - a_{11} a_{22}) u^2 \\ E_3 &= (a_{13} a_{21} - a_{11} a_{23}) z_{GB} u \end{aligned} \quad (3.10)$$

Now, let's assume that we want to place the closed loop poles at $-p_1, -p_2, -p_3, -p_4$ to have the desired system response. Then the desired characteristic equation is,

$$s^4 + \alpha_1 s^3 + \alpha_2 s^2 + \alpha_3 s + \alpha_4 = 0 \quad (3.11)$$

where,

$$\begin{aligned}\alpha_1 &= p_1 + p_2 + p_3 + p_4 \\ \alpha_2 &= p_1 p_2 + p_1 p_3 + p_1 p_4 + p_2 p_3 + p_2 p_4 + p_3 p_4 \\ \alpha_3 &= p_1 p_2 p_3 + p_1 p_2 p_4 + p_1 p_3 p_4 + p_2 p_3 p_4 \\ \alpha_4 &= p_1 p_2 p_3 p_4\end{aligned}\tag{3.12}$$

The feedback gains can now be computed by equating the coefficients of equation 3.9 and 3.11,

$$\begin{aligned}A_2 k_2 + A_3 k_3 &= -\alpha_1 - E_1 \\ B_1 k_2 + B_2 k_2 + B_3 k_3 + B_4 k_4 &= \alpha_2 + E_2 \\ C_1 k_1 + C_2 k_2 + C_4 k_4 &= \alpha_3 + E_3 \\ (D_1 + D_2) k_4 &= \alpha_4\end{aligned}\tag{3.13}$$

We established the method for placing the poles of the system, but we also need to know the desired locations of the poles.

2. Pole Location Selection

In a typical second order system control law design , transient response specifications are given. This results in an allowable region in the s-plane where the desired location of the poles can be obtained. For higher order systems the concept of dominant roots can be employed. In selecting poles the physics of the system must be considered. If the poles are too negative, a small time constant will result, and the system may not be able to react that fast. If we use big gains

K, this also means that the control effort will be large. In practice there are limits based on actuator size and saturation.

Considering the control law design to stabilize the submarine to a level flight path at $\theta = 0$ it is required that the submarine return to the level flight, after some small disturbances in θ or z , within the time it takes for the vehicle to travel three ship lengths. Since our model is 14 feet long and its velocity is 5 feet/sec., the required recovery time is about 10 seconds. This means the time constant is 3 seconds and the closed loop poles should be placed at approximately -0.3 .

After placing the poles using equation 3.13 the control law is found to be,

$$\delta = 0.9917 \theta + 0.8333 w + 0.6026 q - 0.0351 z \quad (3.14)$$

C. FEEDFORWARD CONTROL

The previous discussion on feedback controller assures closed loop stability, but it acts as a regulator in other words takes all the states to zero values. If we have constant disturbances or we want to track some reference value other than zero we can not do this with state feedback alone.

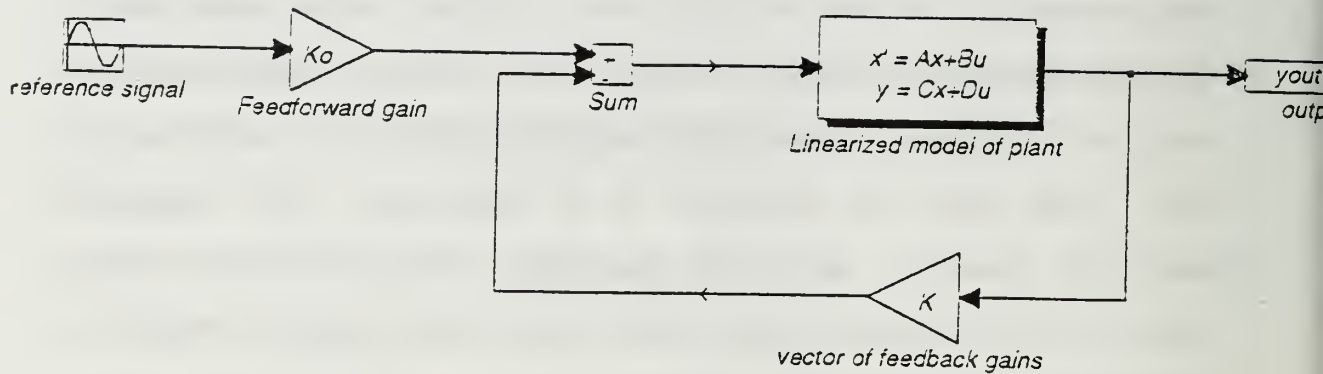


FIGURE 3.1 Feedback and feedforward control application to our linearized model

In the case of non-zero set points or constant disturbances we again need to have the exact same full state feedback to ensure closed loop stability. But we also need to introduce an additional term to our controller in the form

$$u = -Kx + k_o \quad (3.15)$$

where k_0 is the constant feedforward term. k_0 is given as [Ref. 4],

$$k_0 = H_c^{-1}(0) x_0 \quad (3.16)$$

where x_0 is the reference values of the states and $H_c^{-1}(s)$ is the closed loop transfer function,

$$H_c^{-1}(s) = C (sI - A + BK)^{-1} B \quad (3.17)$$

Another way of getting k_0 is looking at the steady state equations of motion. In steady state all the time derivatives in equations 2.1 through 2.4 go to zero and we have,

$$w = \tan \theta_0 \quad (3.18)$$

$$Z_\delta \delta + Z_w w - I_H = 0 \quad (3.19)$$

$$-(x_G - x_B) B \cos \theta_0 - z_{GB} B \sin \theta_0 + M_\delta \delta + M_w w + I_p = 0 \quad (3.20)$$

If the equation 3.19 is multiplied with M_δ and equation 3.20 with Z_δ and set equal to each other and plug in the equation 3.18, we have an equation depending only on θ .

$$(Z_w M_\delta - M_w Z_\delta) \tan \theta_0 + x_G B Z_\delta \cos \theta_0 + z_G B Z_\delta \sin \theta_0 + C_D (E_0 M_\delta - E_1 Z_\delta) \tan \theta_0 |\tan \theta_0| \quad (3.21)$$

Where E_0 and E_1 are the integral terms computed numerically for the Suboff model. The steady state value of θ_0 is found from equation 3.20 by using a Newton-Raphson method in Bifur1 program in the Appendix. Then we can get δ from

equation 3.19,

$$\delta = \frac{I_H - Z_w w}{Z_\delta} = \frac{-C_D E_0 \tan \theta_0 |\tan \theta_0| - Z_w w}{Z_\delta} \quad (3.22)$$

After getting δ , we easily find k_0 from equation 3.15,

$$k_0 = \delta + Kx \quad (3.23)$$

A plot of the steady state angle θ_0 versus x_0 for different values of z_0 is shown in Figure 3.2.

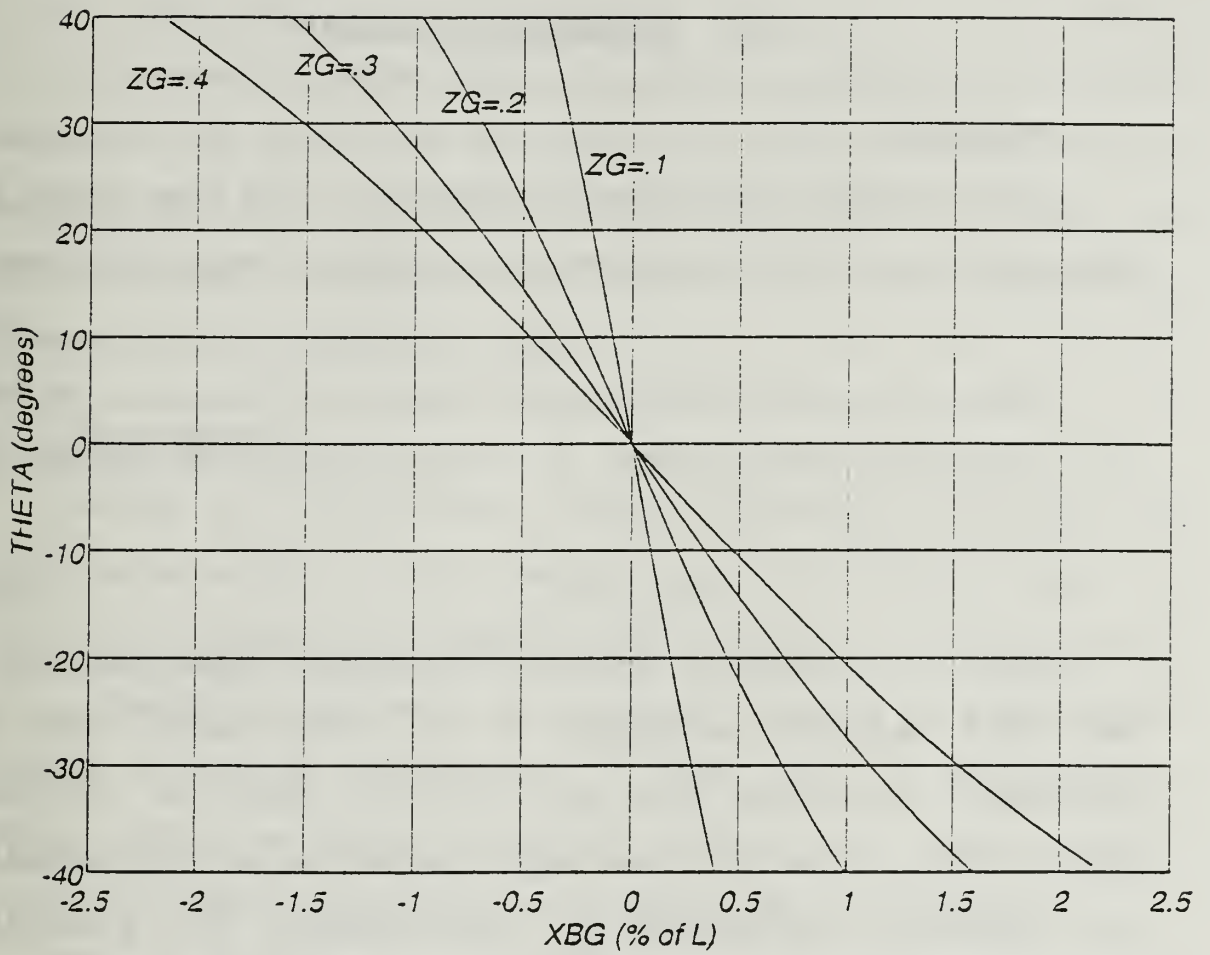


FIGURE 3.2 Steady state pitch angle θ_0 as metacentric height varies

IV. BIFURCATION ANALYSIS

A. STABILITY

The nonlinear equations of motion in the dive plane 2.1 through 2.4 can be expressed in a compact form as follows,

$$\dot{x} = f(x) \quad (4.1)$$

Where x is the state variable vector $x = [\theta, w, q, z]$. We know that the equilibrium points, x_0 of the system are defined by,

$$f(x_0) = 0 \quad (4.2)$$

This is a nonlinear system of algebraic equations and it may have multiple solutions in x_0 , which means that the nonlinear system may have more than one positions of static equilibrium. If we pick one equilibrium, x_0 we can establish its stability properties by linearization. The linearized system becomes,

$$\dot{x} = Ax \quad (4.3)$$

where A is the Jacobian matrix of $f(x)$ evaluated at x_0 ,

$$A = \left. \frac{\partial f}{\partial x} \right|_{x_0} \quad (4.4)$$

and the state has been defined to designate small deviations from the equilibrium x_0 ,

$$x \rightarrow x - x_0 \quad (4.5)$$

In system dynamics as long as all eigenvalues of A have negative real parts, we know that the linear system will be stable. This means that the equilibrium x_0 will be stable for the nonlinear system as well. This is in fact Lyapunov's linearization technique.

B. BIFURCATION

Values of the nonlinear system parameters at which the qualitative nature of the system's motion changes are known as critical or bifurcation values. The phenomena of bifurcation, i.e., quantitative change of parameters leading to qualitative change of system properties, is the topic of bifurcation theory. Euler buckling (Pitchfork bifurcation), limit cycles (Hopf bifurcation) are common examples of bifurcation.

Classical definition of stability states, that the real part of all the eigenvalues of the system must be negative. Therefore, our initial investigations into the stability of the SUBOFF model was to find those eigenvalues whose real parts cross the imaginary axis. We used the bifurcation analysis program, included in the Appendix, to calculate the eigenvalues of the system.

By linearizing the equations of motion, equations 2.1 through 2.4 , the state space equations of the dynamic system can be written in the form,

$$\dot{x} = Ax + Bu \quad (4.5)$$

where,

$$u = -Kx \quad (4.6)$$

and K is the vector of controller gains, as calculated by pole placement in equations 3.13. The eigenvalues of the system are found by solving,

$$\det|A - BK - sI| = 0 \quad (4.7)$$

In the bifurcation program a pseudo-root locus method is employed where the time constant, T_c , is fixed. The constant T_c fixes to placement of the system poles at a given nominal forward speed U_0 and then the model speed, U , is varied incrementally with the system eigenvalues calculated at each speed increment. When the real part of an eigenvalue changes sign between the limits of a speed increment a bisection method is employed to find the speed where the real part of the eigenvalue equals zero.

For each point where the real part of an eigenvalue crosses the imaginary axis the associated T_c and U are plotted on a bifurcation map. This map delineates the regions of

classical stability (all eigenvalues on the left hand plane) from the regions of instability. A family of bifurcation maps were generated by varying nominal speed, U_0 , initial stability, z_{GB} , and longitudinal center of gravity/buoyancy separation, x_{GB} of the submersible.

Figure (4.1) shows a typical bifurcation map with its five distinct regions [Ref. 1]. Region I is the area of classical stability. In region II there is one real positive eigenvalue which is indicative of a pitchfork bifurcation. Pitchfork bifurcations of this model were previously examined by Reidel [Ref. 1]. Regions III, IV, and V have at least one pair of complex conjugate eigenvalues with a positive real part. This would indicate that there should be an unstable oscillatory behavior for the model.

C. RESULTS AND DISCUSSION

The classical stability region in bifurcation maps lies between pitchfork and Hopf bifurcation boundaries. The limits or parameters must be defined for the system designer prior to starting the design. By maximizing the region of stability we can give the designer the most leeway in his work. There are

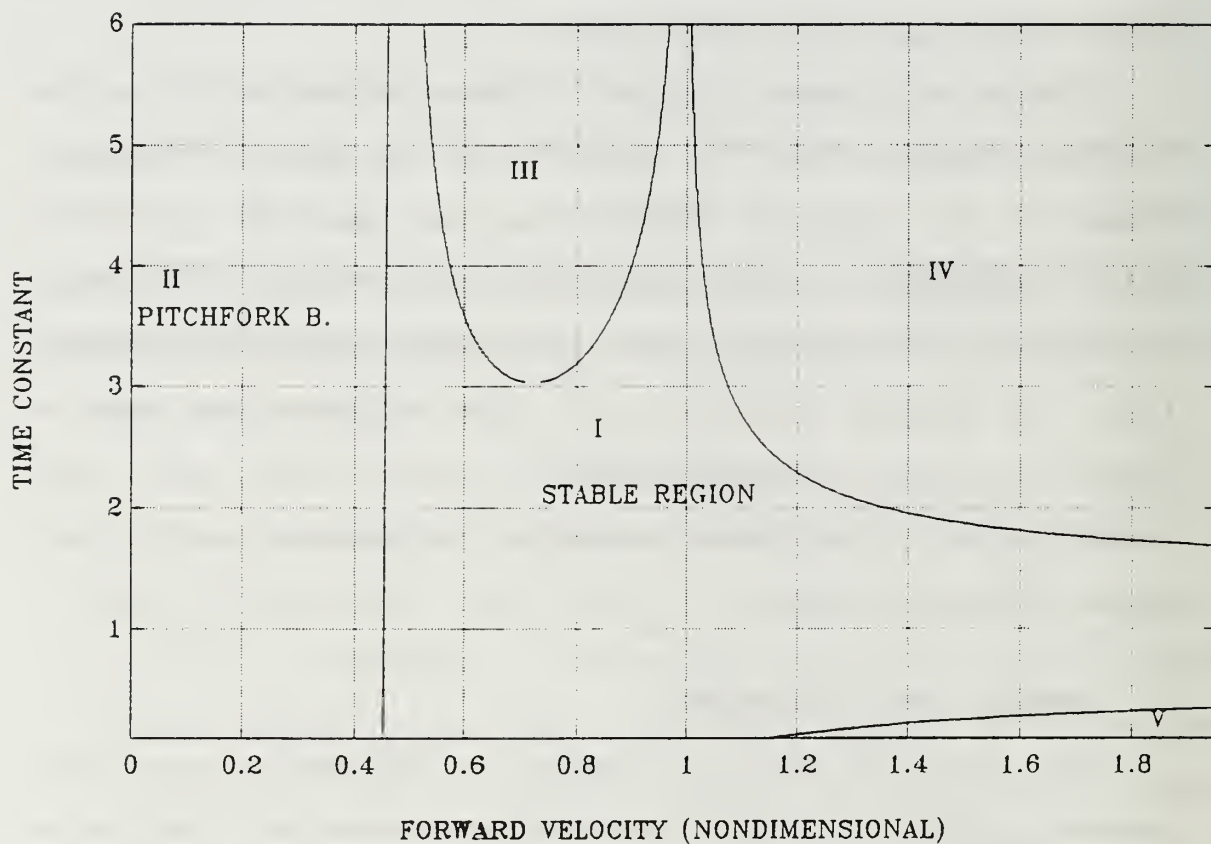


FIGURE 4.1 A typical bifurcation map showing the five distinct regions

two parameters that we used to change the bifurcation maps, the longitudinal separation between center of gravity and center of buoyancy, x_{GB} and the initial stability, z_{GB} .

First we look at the change in x_{GB} . In figures 4.2 through 4.7 we plotted bifurcation curves for different initial stabilities as x_{GB} varies. We can see that as x_{GB} increases the Hopf bifurcation branches H1 and H2 move towards higher speeds and time constants and thus increasing the stability area. The H3 branch however remains constant.

The other important point that we observed is that the system becomes unstable at nominal speed at higher time constants. This is unexpected because we are designing around our nominal speed. A more careful examination in the trimmed case shows that the actual forward velocity becomes, $\sqrt{u^2 + w^2}$. Therefore the system may become stable at a value of u other than nominal.

The next parameter we examined was the initial stability, z_{GB} . Figures 4.8 through 4.14 show the effect of varying z_{GB} from .2 to .4 ft for different x_{GB} values. The H3 branch remains constant while the upper speed H2 branch moves down effectively decreasing the area of stability. The low speed curve H1 moves upwards and increases the low speed area of stability.

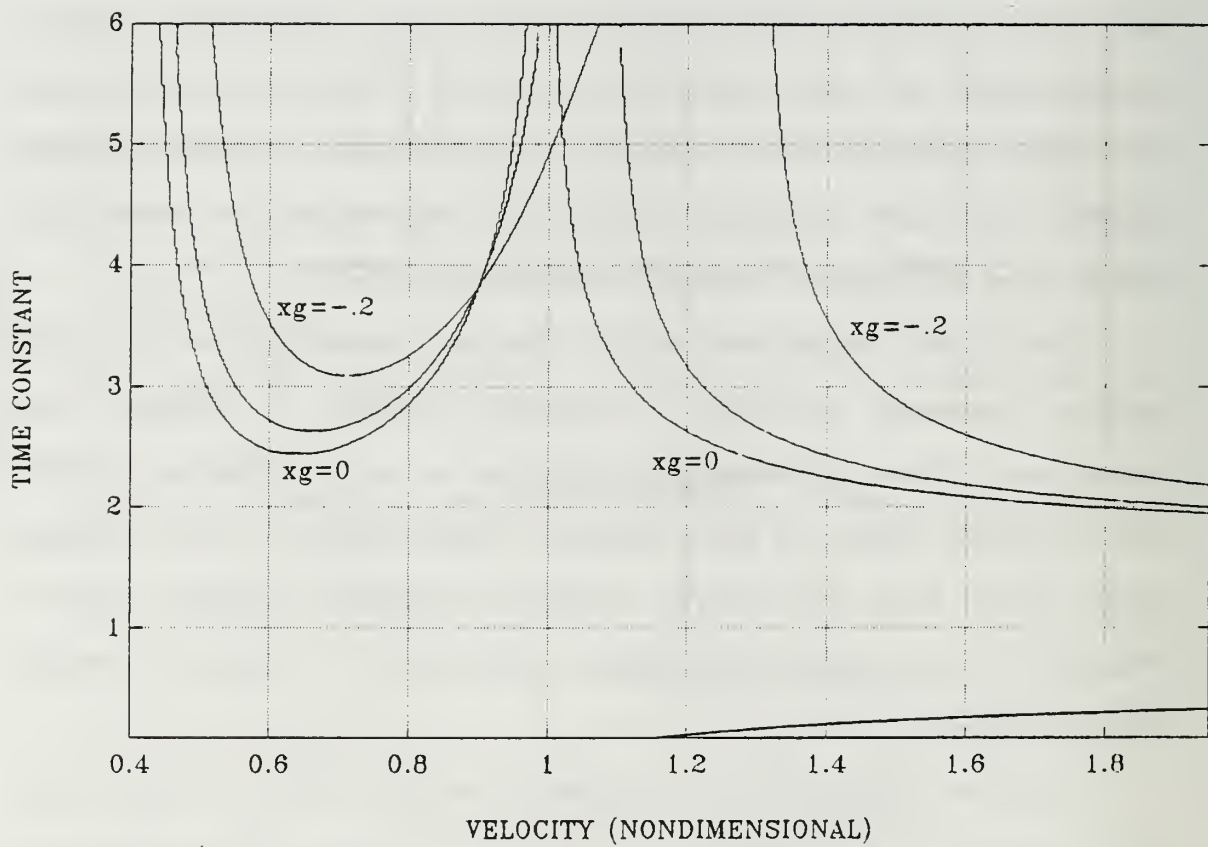


FIGURE 4.2 Bifurcation map as x_g changes between $x_g=0$ and $x_g=-.2$, $z_g=.2$.

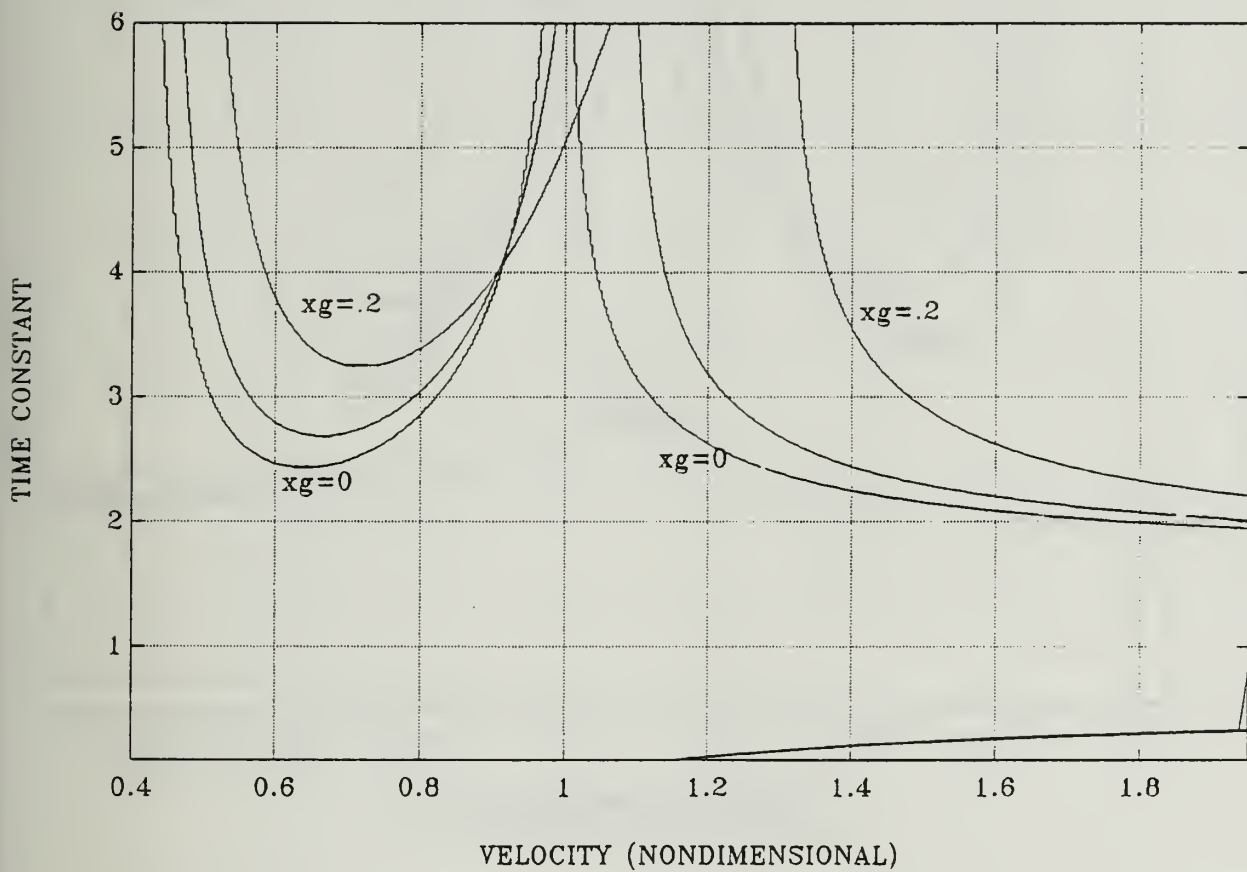


FIGURE 4.3 Bifurcation map as x_g changes between $x_g=0$ and $x_g=.2$, $z_g=.2$.

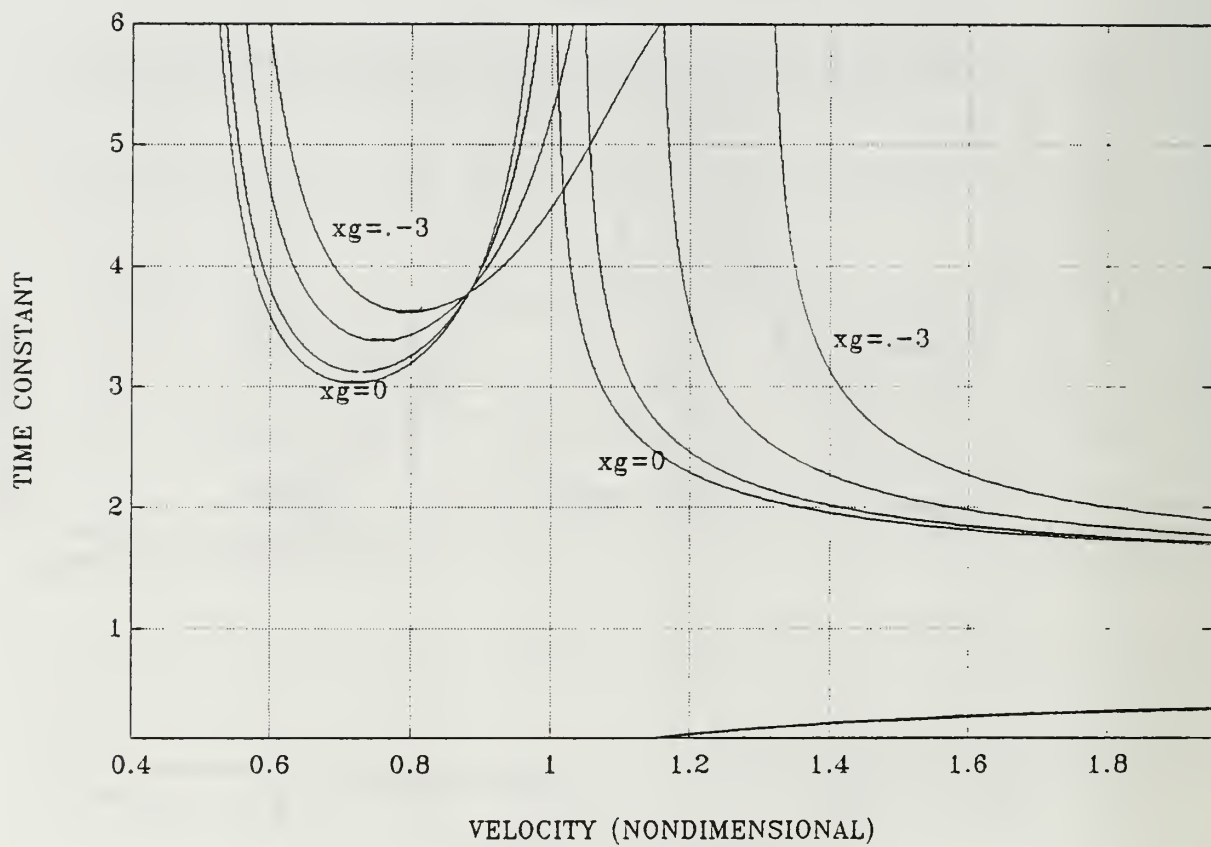


FIGURE 4.4 Bifurcation map as xg changes between $xg=0$ and $xg=-.3$, $zg=.3$.

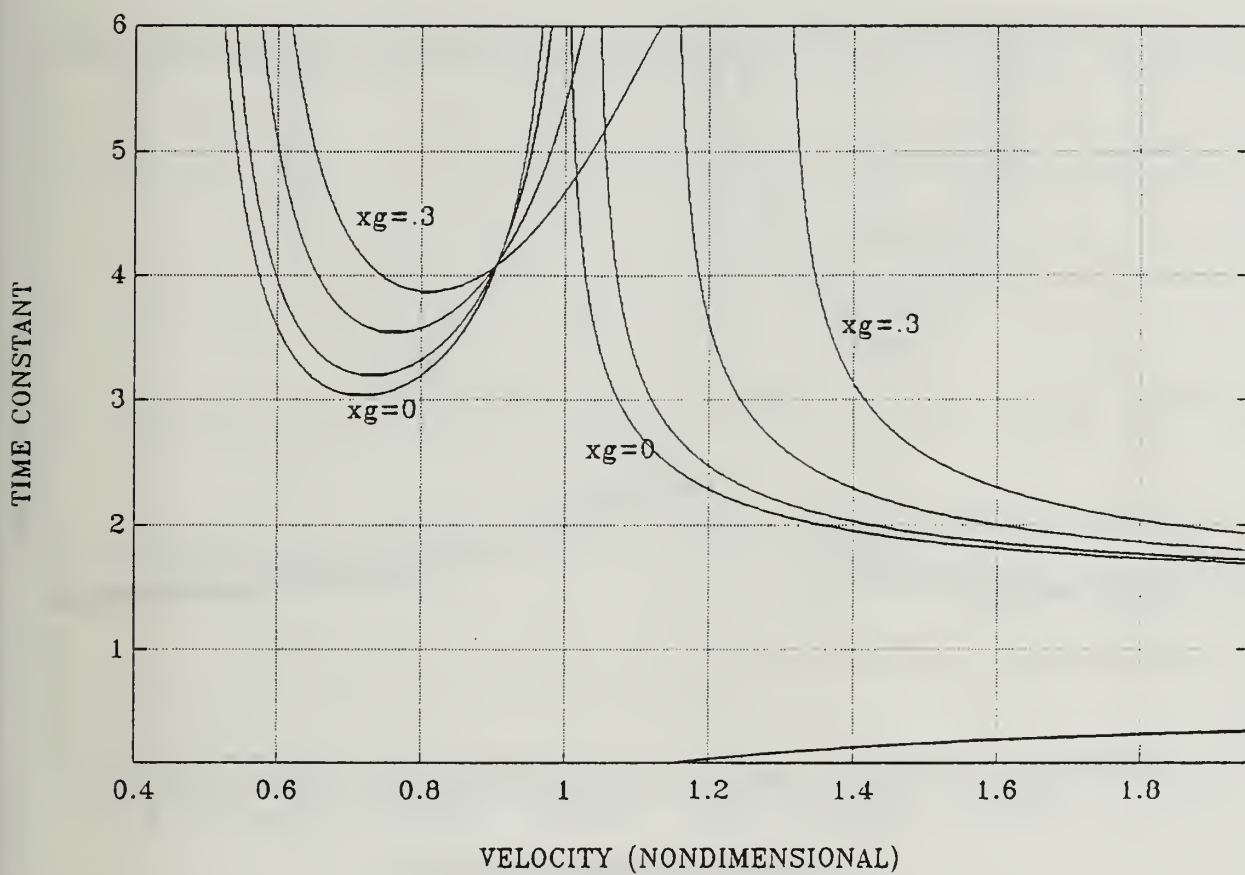


FIGURE 4.5 Bifurcation map as x_g changes between $x_g=0$ and $x_g=.3$, $z_g=.3$.

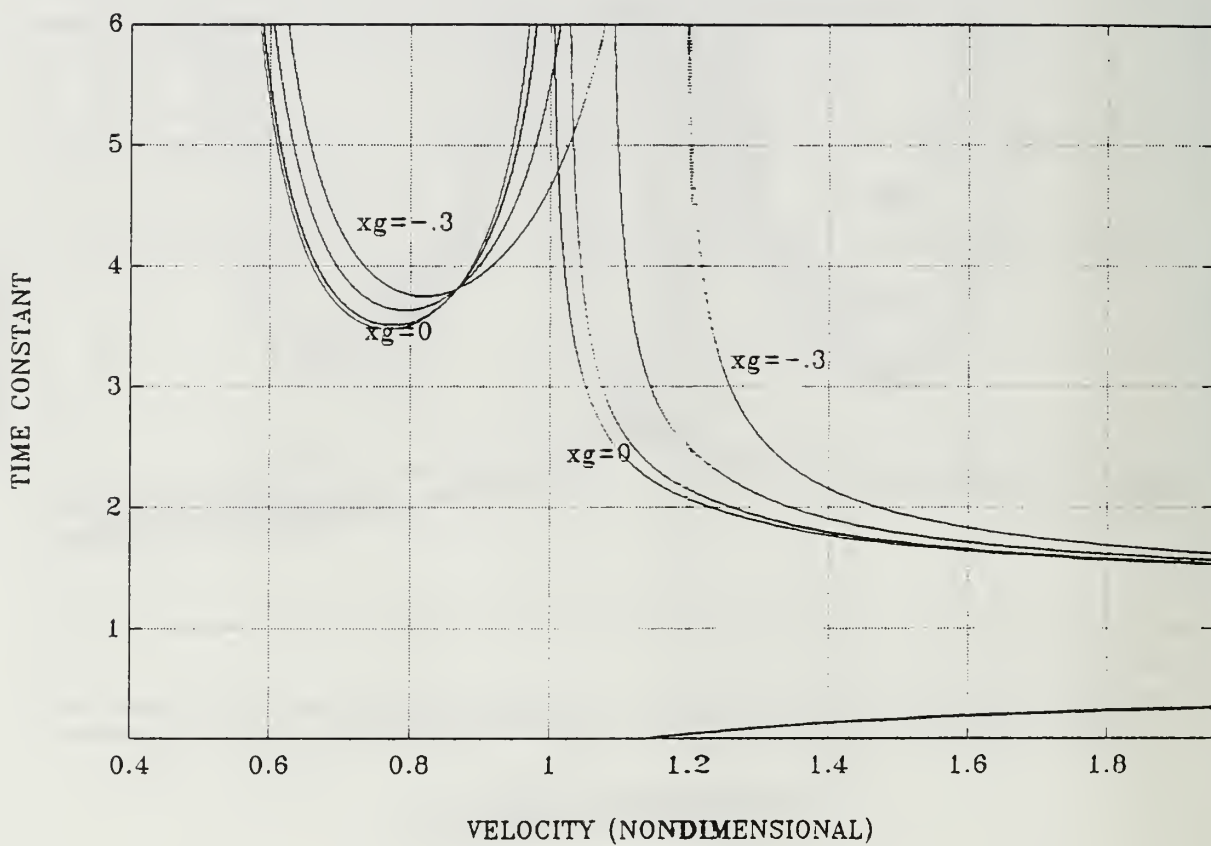


FIGURE 4.6 Bifurcation map as x_g changes between $x_g=0$ and $x_g=-0.3$, $z_g=0.4$.

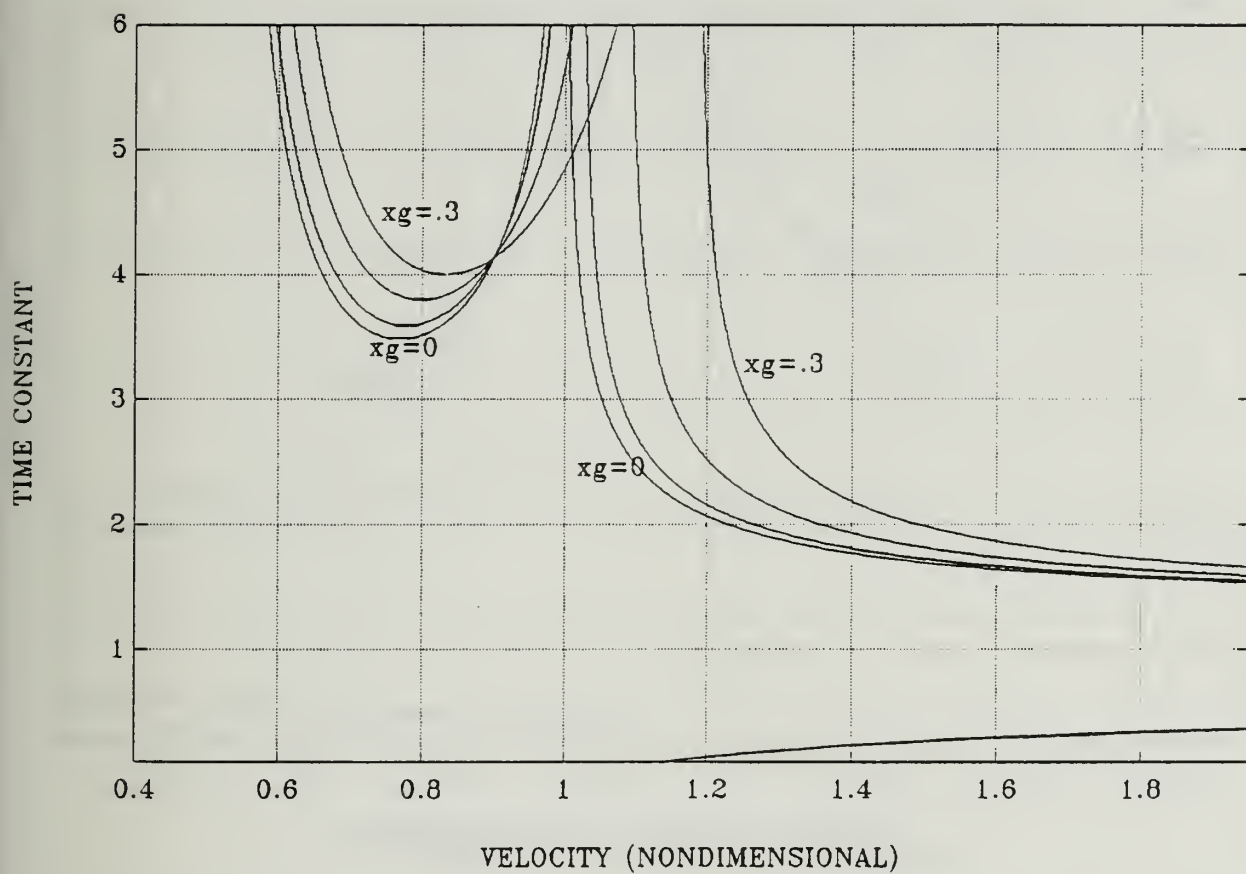


FIGURE 4.7 Bifurcation map as xg changes between $xg=0$ and $xg=.3$, $zg=.4$.

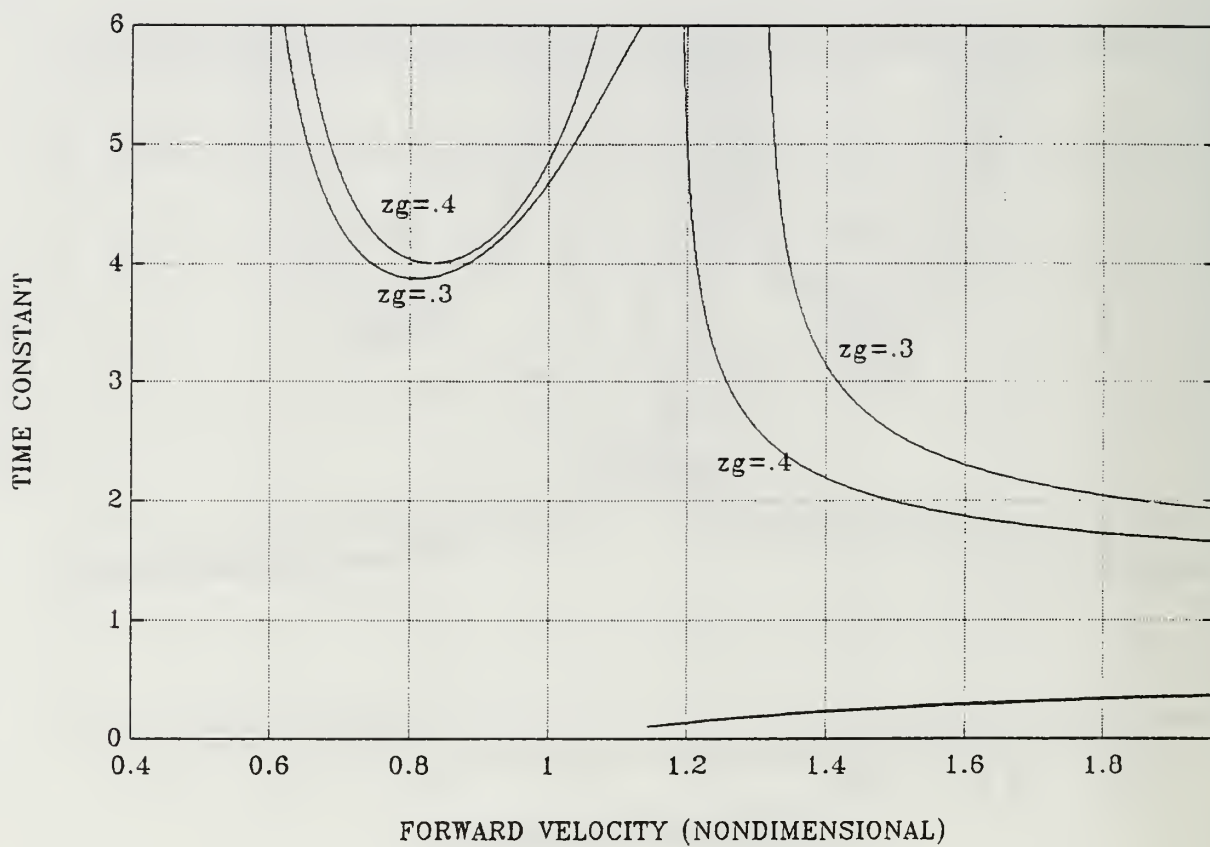


FIGURE 4.8 The effects of changing z_g on the bifurcation maps, $x_g=.3$.

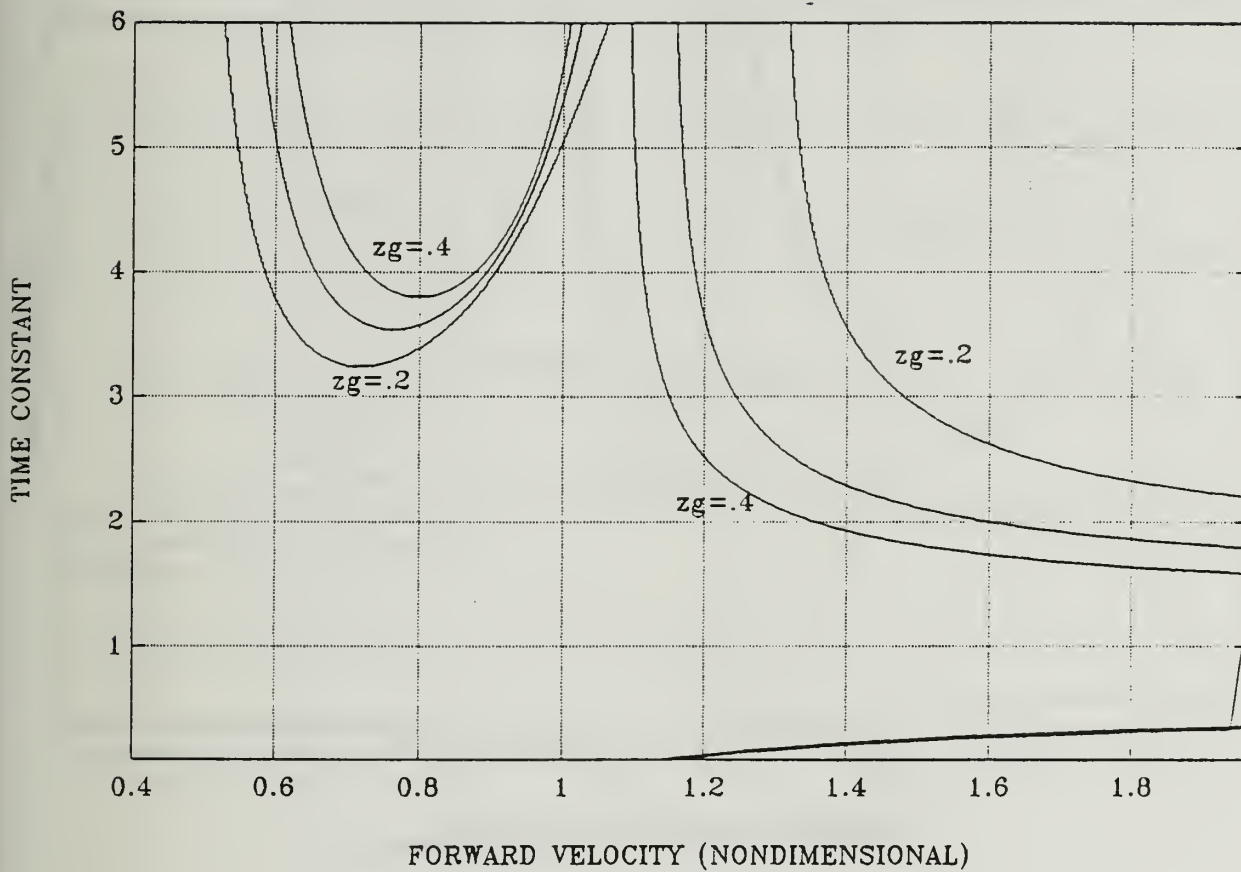


FIGURE 4.9 The effects of changing zg on the bifurcation maps, $xg=.2$.

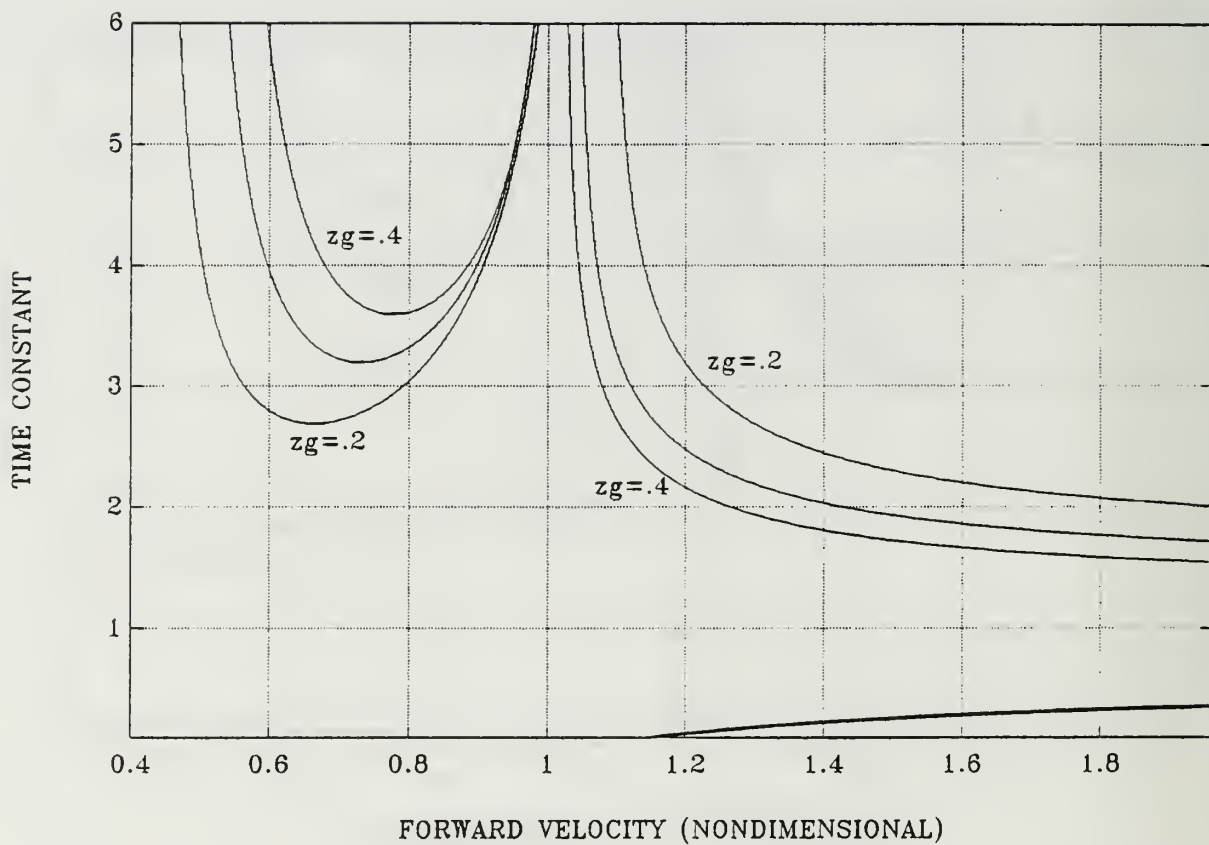


FIGURE 4.10 The effects of changing z_g on the bifurcation maps, $x_g = .1$.

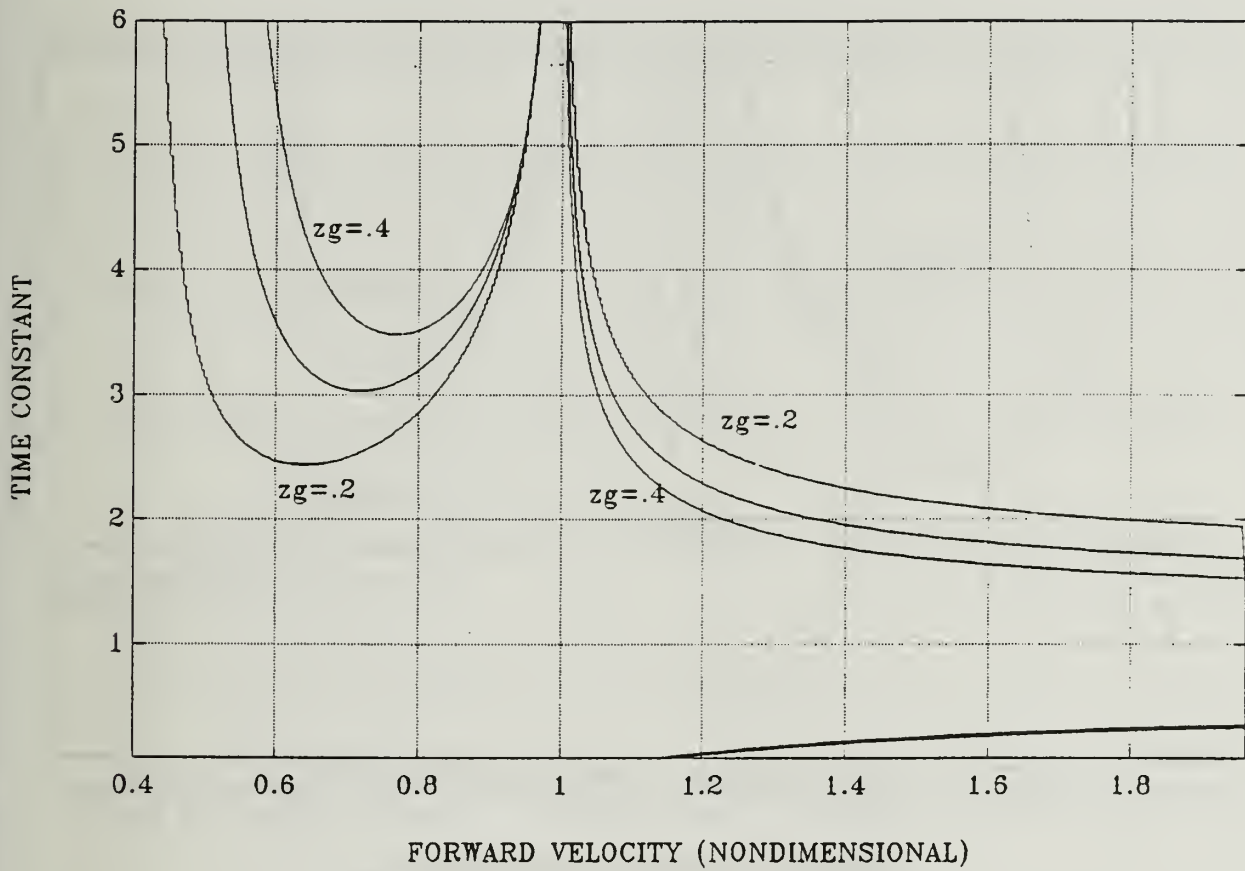


FIGURE 4.11 The effects of changing z_g on the bifurcation maps, $x_g=0$.

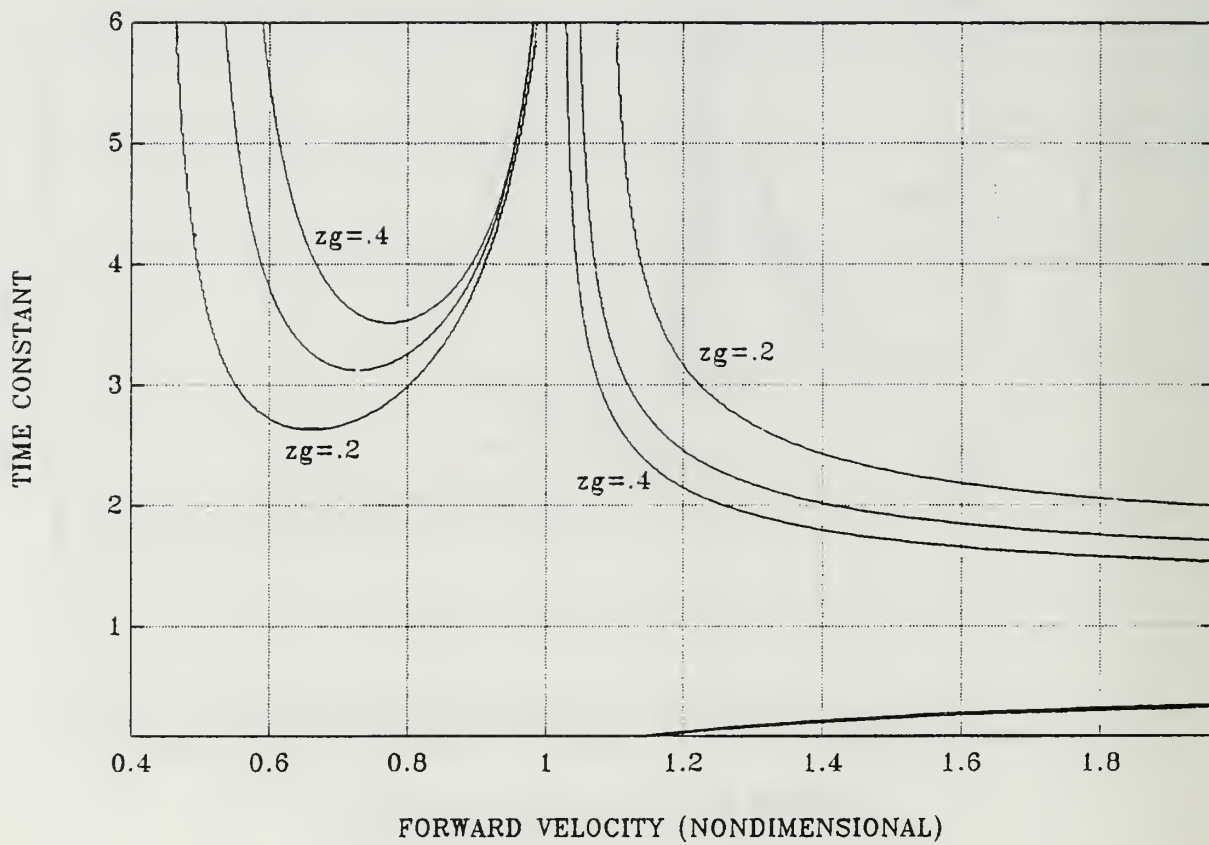


FIGURE 4.12 The effects of changing z_g on the bifurcation maps, $x_g = -.1$.

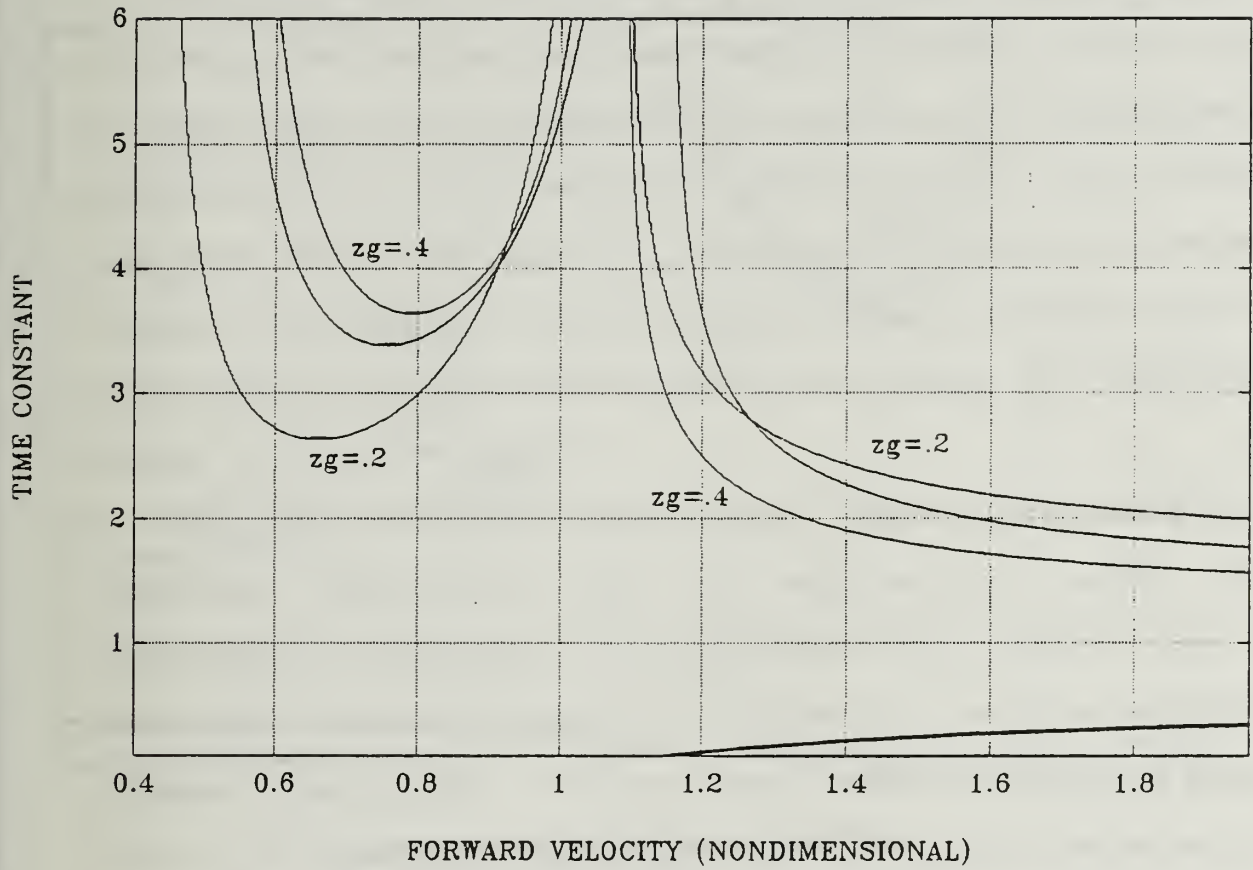


FIGURE 4.13 The effects of changing z_g on the bifurcation maps, $x_g = -.2$.

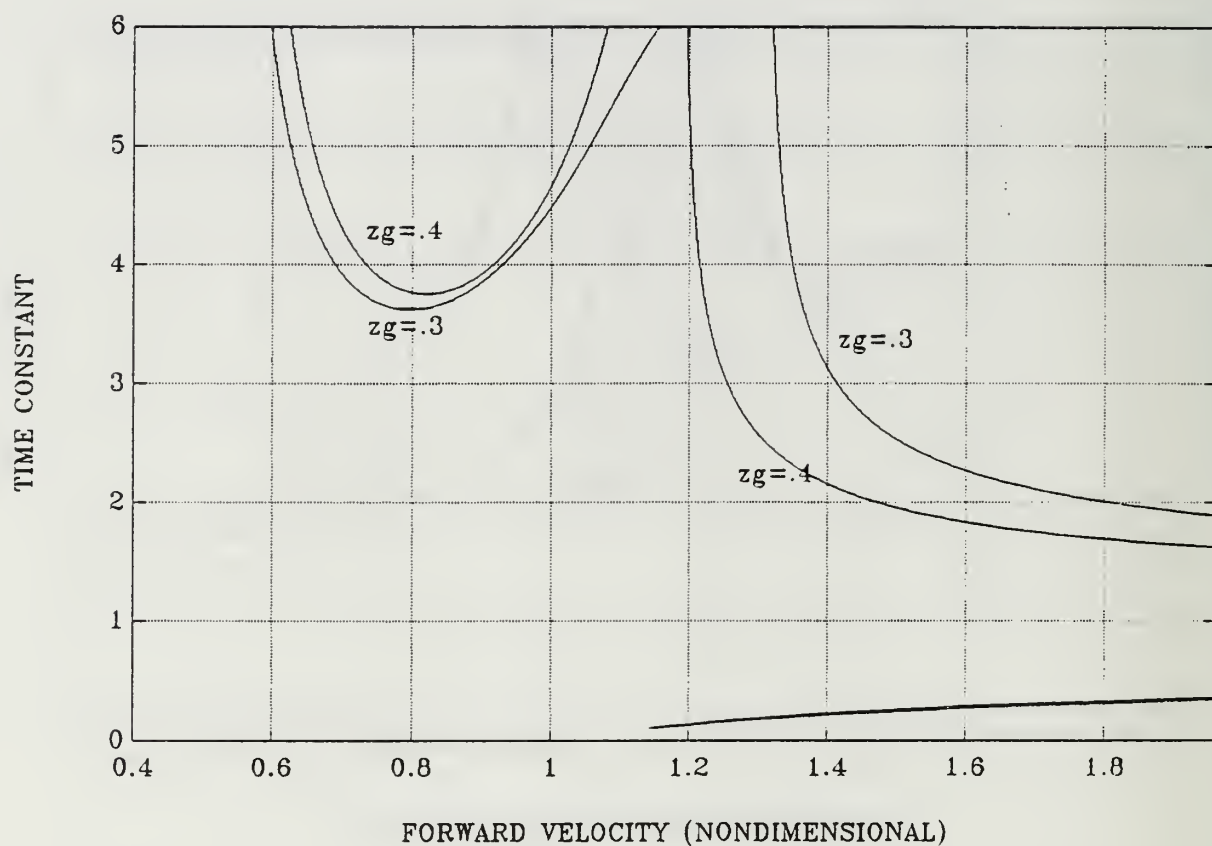


FIGURE 4.14 The effects of changing z_g on the bifurcation maps, $x_g = -.3$.

V. CONCLUSIONS AND RECOMMENDATIONS

A. CONCLUSIONS

Hopf bifurcation analysis is a very useful design tool in the design and evaluation phase. Hopf bifurcation analysis and an identification program that can evaluate the hydrodynamic coefficients for the submersible vehicle will be very useful and save money and time by reducing the amount of model testing. An effective set of control system parameters can be generated in this process that will be optimal for the final design of the submersible.

This type of analysis can set the limits of the ranges of important parameters such as metacentric height and longitudinal separation of buoyancy/gravity centers. As we have seen changes in these two parameters can have dramatic effects on stability. It was found that the moderate speed region of stability increases with increasing metacentric height. The same is not true, however, for high speeds. The longitudinal separation of center of gravity/buoyancy can have a profound effect on stability. It was found that the vehicle may be unstable even at nominal speed. This was attributed to the fact that at high trim angles, the feedback gains which are computed at zero trim, can no longer guarantee stability.

B. RECOMMENDATIONS

The bifurcation analysis program should be expanded to evaluate the performance of the submarine including effects of external forces such as wave effects, currents, and free surface effects.

APPENDIX - BIFURCATION ANALYSIS PROGRAM

```
C  PROGRAM BIFUR1.FOR
C  BIFURCATION ANALYSIS
C  PARAMETERS ARE: TC VS. U
```

```
IMPLICIT DOUBLE PRECISION (A-H,O-Z)
```

```
DOUBLE PRECISION K1,K2,K3,K4,L,MQDOT,MWDOT,MQ,MW,MDS,MDB,MD,
&      MASS,IY,P1,P2,P3,P4,XGB,ZGB
```

```
DIMENSION A(4,4),FV1(4),IV1(4),ZZZ(4,4),WR(4),WI(4),XL(25),
&      BR(25),VEC0(25),VEC1(25),VEC2(25)
```

```
COMMON P1,P2,P3,P4
```

```
C
```

```
OPEN (11,FILE='BIF1.RES',STATUS='NEW')
```

```
OPEN (12,FILE='BIF2.RES',STATUS='NEW')
```

```
OPEN (13,FILE='BIF3.RES',STATUS='NEW')
```

```
C NUMERIC INFO OF DARPA SUBOFF MODEL
```

```
WEIGHT=1556.2363
```

```
BUO  =1556.2363
```

```
L    =13.9792
```

```
IY   =561.32
```

```
G    =32.2
```

```
MASS =WEIGHT/G
```

```
RHO  =1.94
```

```
XB   =0.0
```

```
ZB   =0.0
```

```
CD   =0.4
```

CD =0.5*CD*RHO

C

WRITE (*,*) 'ENTER MIN, MAX, AND INCREMENTS IN Tc (nondim)'

READ (*,*) TCMIN,TCMAX,ITC

WRITE (*,*) 'ENTER MIN, MAX, AND INCREMENTS IN U (nondim)'

READ (*,*) UMIN,UMAX,IU

C WRITE (*,*) 'ENTER NOMINAL SPEED'

C READ (*,*) U0

WRITE (*,*) 'ENTER XG AND ZG'

READ (*,*) XG,ZG

U0=9

C

ZGB=ZG-ZB

XGB=XG-XB

TCMIN=TCMIN*L/U0

TCMAX=TCMAX*L/U0

UMIN =UMIN*U0

UMAX =UMAX*U0

C HYDRODYNAMIC COEFFICIENTS

ZQDOT=-6.3300E-04*0.5*RHO*L**4

ZWDOT=-1.4529E-02*0.5*RHO*L**3

ZQ = 7.5450E-03*0.5*RHO*L**3

ZW =-1.3910E-02*0.5*RHO*L**2

ZDS =-5.6030E-03*0.5*RHO*L**2

ZDB =-5.6030E-03*0.5*RHO*L**2

MQDOT=-8.8000E-04*0.5*RHO*L**5

MWDOT=-5.6100E-04*0.5*RHO*L**4

$$MQ = -3.7020E-03 * 0.5 * RHO * L^{**4}$$

$$MW = 1.0324E-02 * 0.5 * RHO * L^{**3}$$

$$MDS = -2.4090E-03 * 0.5 * RHO * L^{**3}$$

$$MDB = 2.4090E-03 * 0.5 * RHO * L^{**3}$$

$$XL(1)=0.0$$

$$XL(2)=0.1$$

$$XL(3)=0.2$$

$$XL(4)=0.3$$

$$XL(5)=0.4$$

$$XL(6)=0.5$$

$$XL(7)=0.6$$

$$XL(8)=0.7$$

$$XL(9)=1.0$$

$$XL(10)=2.0$$

$$XL(11)=3.0$$

$$XL(12)=4.0$$

$$XL(13)=7.7143$$

$$XL(14)=10.0$$

$$XL(15)=15.1429$$

$$XL(16)=16.0$$

$$XL(17)=17.0$$

$$XL(18)=18.0$$

$$XL(19)=19.0$$

$$XL(20)=20.0$$

$$XL(21)=20.1$$

XL(22)=20.2

XL(23)=20.3

XL(24)=20.4

XL(25)=20.4167

DO 102 N=1,25

XL(N) = (L/20.)*XL(N) - L/2.

102 CONTINUE

BR(1)=0.0

BR(2)=0.485

BR(3)=0.658

BR(4)=0.778

BR(5)=0.871

BR(6)=0.945

BR(7)=1.010

BR(8)=1.060

BR(9)=1.18

BR(10)=1.41

BR(11)=1.57

BR(12)=1.66

BR(13)=1.67

BR(14)=1.67

BR(15)=1.67

BR(16)=1.63

BR(17)=1.37

BR(18)=0.919

BR(19)=0.448

BR(20)=0.195

```

BR(21)=0.188
BR(22)=0.168
BR(23)=0.132
BR(24)=0.053
BR(25)=0.0
DO 104 K=1,25
    VEC0(K)=BR(K)
    VEC1(K)=XL(K)*BR(K)
    VEC2(K)=XL(K)*XL(K)*BR(K)
104 CONTINUE
    CALL TRAP(25,VECO,XL,EO)
    CALL TRAP(25,VEC1,XL,E1)
    CALL TRAP(25,VEC2,XL,E2)
C
    ALPHA=0.0
    ZD=ZDS+ALPHA*ZDB
    MD=MDS+ALPHA*MDB

C  CALCULATING THE SS PITCH ANGLE  $\theta_0$ 
C  WITH NEWTON RAPHSON METHOD
    P1= ZW*MD - MW*ZD
    P2= XG*BUO*ZD
    P3= ZG*BUO*ZD
    P4= CD*(MD*E0 - ZD*E1)
    WRITE(*,*) P1,P2,P3,P4
    EPSI=.00000001
    THETA0=0

```



```

      IF(XGB.GT.0) P4=-1*P4
18   DO 19 I=1,2000
      FT=FUNC(THETA0)
      DFT=DFUNC(THETA0)
      DELT=FT/DFT
      THETA0=THETA0-DELT
      IF(ABS(DELT)-EPSI) 20,20,19
19   CONTINUE
      FT=FUNC(THETA0)
20   WRITE(*,*) THETA0 , FT
C
      DV=(MASS-ZWDOT)*(IY-MQDOT)-(MASS*XG+ZQDOT)*(MASS*XG+MWDOT)
      A11DV=(IY-MQDOT)*(ZW-2*CD*EO*U*TAN(THETA0))
      &    +(MASS*XG+ZQDOT)*(MW+2*CD*E1*U*TAN(THETA0))

      A12DV=(IY-MQDOT)*(MASS+ZQ+2*CD*E1*U*TAN(THETA0))+
      &    (MASS*XG+ZQDOT)
      &    *(MQ-MASS*XG-MASS*ZG*U*TAN(THETA0)-2*CD*E2*U*TAN(THETA0))
      A13DV=-(MASS*XG+ZQDOT)*WEIGHT
      B1DV =(IY-MQDOT)*ZD+(MASS*XG+ZQDOT)*MD
      A21DV=(MASS-ZWDOT)*(MW+2*CD*E1*U*TAN(THETA0))
      &    +(MASS*XG+MWDOT)*(ZW-2*CD*EO*U*TAN(THETA0))

      A22DV=(MASS-ZWDOT)*(MQ-MASS*XG-MASS*ZG*U*TAN(THETA0)-2*CD*E2*U
      &    *TAN(THETA0))+(MASS*XG+MWDOT)*
      &    (MASS+ZQ+2*CD*E1*U*TAN(THETA0))
      A23DV=-(MASS-ZWDOT)*WEIGHT

```

$$B2DV = (MASS - ZWDOT) * MD + (MASS * XG + MWDOT) * ZD$$

C

$$A11 = A11DV / DV$$

$$A12 = A12DV / DV$$

$$A13 = A13DV / DV$$

$$A21 = A21DV / DV$$

$$A22 = A22DV / DV$$

$$A23 = A23DV / DV$$

$$B1 = B1DV / DV$$

$$B2 = B2DV / DV$$

C

$$EPS = 1.D-5$$

$$ILMAX = 1500$$

C

$$DO 1 I=1, ITC$$

$$WRITE (*, 2001) I, ITC$$

$$TC = TCMIN + (I-1) * (TCMAX - TCMIN) / (ITC-1)$$

$$POLE = 1.0 / TC$$

$$ALPHA3 = 4.0 * POLE$$

$$ALPHA2 = 6.0 * POLE ** 2$$

$$ALPHA1 = 4.0 * POLE ** 3$$

$$ALPHA0 = POLE ** 4$$

$$K4 = ALPHA0 / ((B1 * A21 - B2 * A11) * U0 ** 4 + (B1 * A23 - B2 * A13) * ZGB * U0 ** 2)$$

$$A2M = B1 * U0 ** 2$$

$$A3M = B2 * U0 ** 2$$

$$A0M = -(A11 + A22) * U0 - ALPHA3$$

$$B1M = B2 * U0 ** 2$$

$$B2M=(B2*A12-B1*A22)*U0**3$$

$$B3M=(B1*A21-B2*A11)*U0**3$$

$$B0M=(A11*A22-A21*A12)*U0**2-A23*ZGB-ALPHA2-B1*U0*U0*K4$$

$$C1M=(B2*A11-B1*A21)*U0**3$$

$$C2M=(B1*A23-B2*A13)*ZGB*U0**2$$

$$C0M=(A13*A21-A23*A11)*ZGB*U0+ALPHA1-(B2+B1*A22-B2*A12)*K4*U0**3$$

$$K2=C1M*B0M*A3M-B1M*C0M*A3M-C1M*B3M*A0M$$

$$K2=K2/(C1M*B2M*A3M-B1M*C2M*A3M-C1M*B3M*A2M)$$

$$K1=(C0M-C2M*K2)/C1M$$

$$K3=(A0M-A2M*K2)/A3M$$

C

DO 2 J=1,IU

$$U=UMIN+(J-1)*(UMAX-UMIN)/(IU-1)$$

$$A(1,1)=0.0D0$$

$$A(1,2)=0.0D0$$

$$A(1,3)=1.0D0$$

$$A(1,4)=0.0D0$$

$$A(2,1)=-A13*(XGB*SIN(THETA0)-ZGB*COS(THETA0))+B1*U*U*K1$$

$$A(2,2)=A11*U +B1*U*U*K2$$

$$A(2,3)=A12*U +B1*U*U*K3$$

$$A(2,4)= B1*U*U*K4$$

$$A(3,1)=-A23*(XGB*SIN(THETA0)-ZGB*COS(THETA0))+B2*U*U*K1$$

$$A(3,2)= A21*U +B2*U*U*K2$$

$$A(3,3)= A22*U +B2*U*U*K3$$

$$A(3,4)= B2*U*U*K4$$

$$A(4,1)=- U$$

$$A(4,2)= 1.0D0$$

A(4,3)= 0.0D0

A(4,4)= 0.0D0

C

CALL RG(4,4,A,WR,WI,0,ZZZ,IV1,FV1,IERR)

CALL DSTABL(DEOS,WR,WI,FREQ)

C

IF (J.GT.1) GO TO 10

DEOSOO= DEOS

UOO = U

LL= 0

GO TO 2

10 DEOSNN = DEOS

UNN = U

PR= DEOSNN*DEOSOO

IF (PR.GT.0.D0) GO TO 3

LL = LL+1

IF (LL.GT.3) STOP 1000

IL = 0

UO = UOO

UN = UNN

DEOSO = DEOSOO

DEOSN = DEOSNN

6 UL = UO

UR = UN

DEOSL = DEOSO

DEOSR = DEOSN

C U = (UL+UR)/2.D0

```

ALPHA = (DEOSL-DEOSR)/(UL-UR)
U =- (DEOSL-ALPHA*UL)/ALPHA
A(1,1) = 0.0D0
A(1,2) = 0.0D0
A(1,3) = 1.0D0
A(1,4) = 0.0D0
A(2,1) = A13*(XGB*SIN(THETAO)-ZGB*COS(THETAO))+B1*U*U*K1
A(2,2) = A11*U +B1*U*U*K2
A(2,3 )= A12*U +B1*U*U*K3
A(2,4 )= B1*U*U*K4
A(3,1) = A23*(XGB*SIN(THETAO)-ZGB*COS(THETAO))+B2*U*U*K1
A(3,2) = A21*U +B2*U*U*K2
A(3,3) = A22*U +B2*U*U*K3
A(3,4 )= B2*U*U*K4
A(4,1) =- U
A(4,2) = 1.0D0
A(4,3) = 0.0D0
A(4,4 )= 0.0D0

```

C

```

CALL RG(4,4,A,WR,WI,0,ZZZ,IV1,FV1,IERR)
CALL DSTABL(DEOS,WR,WI,FREQ)

```

C

```

DEOSM = DEOS
UM = U
PRL = DEOSL*DEOSM
PRR = DEOSR*DEOSM
IF (PRL.GT.0.D0) GO TO 5

```

```

    UO = UL
    UN = UM
    DEOSO = DEOSL
    DEOSN = DEOSM
    IL = IL+1
    IF (IL.GT.ILMAX) STOP 3100
    DIF = DABS(UL-UM)
    IF (DIF.GT.EPS) GO TO 6
    U = UM
    GO TO 4
5   IF (PRR.GT.0.D0) STOP 3200
    UO = UM
    UN = UR
    DEOSO = DEOSM
    DEOSN = DEOSR
    IL = IL+1
    IF (IL.GT.ILMAX) STOP 3100
    DIF = DABS(UM-UR)
    IF (DIF.GT.EPS) GO TO 6
    U = UM
4   LLL = 10+LL
    WRITE (LLL,*) U/U0,TC*U0/L
3   UOO = UNN
    DEOSOO = DEOSNN
2   CONTINUE
1   CONTINUE
C

```

2001 FORMAT (2I5)

END

SUBROUTINE DSTABL(DEOS,WR,WI,OMEGA)

IMPLICIT DOUBLE PRECISION (A-H,O-Z)

DIMENSION WR(4),WI(4)

DEOS=-1.0D+20

DO 1 I = 1,4

IF (WR(I).LT.DEOS) GO TO 1

DEOS = WR(I)

IJ = I

1 CONTINUE

OMEGA = WI(IJ)

OMEGA = DABS(OMEGA)

RETURN

END

C

SUBROUTINE TRAP(N,A,B,OUT)

C NUMERICAL INTEGRATION ROUTINE USING THE TRAPEZOIDAL RULE

IMPLICIT DOUBLE PRECISION (A-H,O-Z)

DIMENSION A(1),B(1)

N1 = N-1

OUT = 0.0

DO 1 I = 1,N1

OUT1 = 0.5*(A(I)+A(I+1))*(B(I+1)-B(I))

OUT = OUT+OUT1

1 CONTINUE

RETURN

END

C FUNCTIONS USED IN NEWTON RAPHSON ROUTINE

FUNCTION FUNC(THETA0)

IMPLICIT DOUBLE PRECISION (A-H,O-Z)

COMMON P1,P2,P3,P4

FUNC = P1*DTAN(THETA0) + P2*DCOS(THETA0) + P3*DSIN(THETA0)

& + P4*(DTAN(THETA0))**2

RETURN

END

FUNCTION DFUNC(THETA0)

IMPLICIT DOUBLE PRECISION (A-H,O-Z)

COMMON P1,P2,P3,P4

DFUNC= P1*(1.D0/DCOS(THETA0))**2 - P2*DSIN(THETA0) +

& P3*DCOS(THETA0) + P4*2.D0*DTAN(THETA0)*(1.D0/DCOS(THETA0))**2.D0

RETURN

END

LIST OF REFERENCES

1. Bateman, C.A., (December 1993) Hopf Bifurcation Analysis for Depth Control of Submersible Vehicles. Master's Thesis, Department of Mechanical Engineering, Naval Postgraduate School.
2. Riedel, J.S., (June 1993) Pitchfork Bifurcations and Dive Plane Reversal of Submarines at Low Speeds. Master's Thesis, Department of Mechanical Engineering, Naval Postgraduate School.
3. Stewart, H.B., and Thompson, J.M.T., (1986) Nonlinear Dynamics and Chaos, Geometrical Methods for Engineers and Scientists. John Wiley and Sons, New York.
4. Kwakernaak, H. and Sivan, R., (1972) Linear Optimal Control Systems. John Wiley and Sons, New York.
5. Fossen, T.I., (1987) Nonlinear Modelling and Control of Underwater Vehicles. Doctoral Thesis, Division of Engineering, Cybernetics, Department of Electrical Engineering, Norwegian Institute of Technology.
6. Roddy, R.F. (1990) Investigation of the Stability and Control Characteristics of Several Configurations of the DARPA SUBOFF Model (DRTC mODEL 5470) from captive-model experiments. DAVID Taylor research center, Report DRTC/SHD-1298-08.

INITIAL DISTRIBUTION LIST

	No. Copies
1. Defence Technical Information Center Cameron Station Alexandria VA 22304-6145	2
2. Library, Code 052 Naval Postgraduate School Monterey CA 93943-5002	2
3. Deniz Harp Okulu Tuzla Istanbul, TURKEY	2
4. Golcuk Tersanesi Komutanligi Golcuk Kocaeli, TURKEY	2
5. Taskizak Tersanesi Komutanligi Kasimpasa Istanbul, TURKEY	2
6. Deniz Kuvvetleri Komutanligi Personel Egitim Daire Baskanligi Bakanliklar Ankara, TURKEY	1
7. Professor Fotis A. Papoulias, Code ME/Pa Department of Mechanical Engineering Naval Postgraduate School Monterey, CA 93943-5100	1
8. Department Chairman, Code ME/Kk Department of Mechanical Engineering Naval Postgraduate School Monterey, CA 93943-5100	1

9. Naval Engineering Curricular Office, Code 34 1
Naval Postgraduate School
Monterey, CA 93943-5100
10. Selcuk Ornek 1
Korfez cad. No: 27-A/9
Derince, Kocaeli
41900, TURKEY

DUDLEY KNOX LIBRARY
NAVAL POSTGRADUATE SCHOOL
MONTEREY CA 93943-5101



GAYLORD 5

DUDLEY KNOX LIBRARY



3 2768 00308428 6